The Journal of Immunology

Dual Oxidase 1 Induced by Th2 Cytokines Promotes STAT6 Phosphorylation via Oxidative Inactivation of Protein Tyrosine Phosphatase 1B in Human Epidermal Keratinocytes

Satoshi Hirakawa, Rumiko Saito, Hiroshi Ohara, Ryuhei Okuyama and Setsuya Aiba

J Immunol 2011; 186:4762-4770; Prepublished online 16 March 2011;
doi: 10.4049/jimmunol.1000791
http://www.jimmunol.org/content/186/8/4762

The Journal of Immunology is published twice each month by
The American Association of Immunologists, Inc.,
1451 Rockville Pike, Suite 650, Rockville, MD 20852

Print ISSN: 0022-1767 Online ISSN: 1550-6606.

Dual Oxidase 1 Induced by Th2 Cytokines Promotes STAT6 Phosphorylation via Oxidative Inactivation of Protein Tyrosine Phosphatase 1B in Human Epidermal Keratinocytes

Satoshi Hirakawa,*,† Rumiko Saito,* Hiroshi Ohara,‡ Ryuhei Okuyama,*,[1] and Setsuya Aiba*

Although hydrogen peroxide (H_2O_2) is better known for its cytotoxic effects, in recent years it has been shown to play a crucial role in eukaryotic signal transduction. In respiratory tract epithelial cells, the dual oxidase (DUOX) proteins 1 and 2 has been identified as the cellular source of H_2O_2. However, the expression of DUOX1 or DUOX2 has not yet been examined in keratinocytes. In this study, using a DNA microarray, we demonstrated that, of the seven NOX/DUOX family members in normal human epidermal keratinocytes (NHEK), IL-4/IL-13 treatment augments the expression of only DUOX1 mRNA. We next confirmed the IL-4/IL-13 induction of DUOX1 in NHEK at the mRNA and protein level using quantitative real-time PCR and Western blotting, respectively. In addition, we demonstrated that this augmented DUOX1 expression was accompanied by increased H_2O_2 production, which was significantly suppressed both by diphenyleneiodonium, an inhibitor of NADPH oxidase, and by small interfering RNA against DUOX1. Finally, we demonstrated that the increased expression of DUOX1 in IL-4/IL-13–treated NHEK augments STAT6 phosphorylation via oxidative inactivation of protein tyrosine phosphatase 1B. These results revealed a novel role of IL-4/IL-13–induced DUOX1 expression in making a positive feedback loop for IL-4/IL-13 signaling in keratinocytes. ***The Journal of Immunology*****, 2011, 186: 4762–4770.**

Physiological generation of reactive oxygen species (ROS) can occur as a by-product of other biological reactions. ROS is generated as a by-product by mitochondria, peroxisomes, cytochrome P450, and other cellular elements. However, the phagocyte NADPH oxidase, gp91phox, which is also called NOX2 using the novel NOX terminology, is the first identified example of an enzyme that generates ROS not as a by-product, but rather as the primary function of the enzyme. The discovery of other members of the NOX family of NADPH oxidases demonstrated that enzymes whose primary function is ROS generation are not limited to phagocytes. In fact, ROS-generating enzymes are found in virtually every tissue. ROS is generally generated by a cascade of reactions that starts with the production of superoxide. Superoxide rapidly dismutates to hydrogen peroxide (H_2O_2) either spontaneously, particularly at low pH, or after catalysis by superoxide dismutase [reviewed by Bedard and Krause (1)].

Several homologs of the gp91phox NADPH oxidase subunit of phagocytes have been identified and form the NOX gene family (reviewed by Lambeth [2]). An evolutionary tree has been constructed for this family, in which three subgroups have been proposed for classification of the NOX family members (reviewed by Lambeth [3]). One group comprises NOX1, NOX2 (gp91phox), NOX3, and NOX4, which all have in common a similar molecular mass (~65 kDa). Another subgroup consists of the dual oxidase (DUOX) 1 and 2, which are characterized by an additional N-terminal peroxidase domain and two EF-hand Ca^{2+}-binding domains. Finally, NOX5 is divergent from the other members and forms the third group.

DUOX proteins have been identified as the cellular source of H_2O_2 in respiratory tract epithelial cells (4–7). Moreover, Harper et al. (8) have shown that the expression of DUOX1 and DUOX2 is differentially regulated by Th1 and Th2 cytokines in airway epithelium. In keratinocytes, however, although it is known that NOX1, NOX2, and NOX4 are expressed at the mRNA and/or protein level (9–11), the expression of DUOX1 or DUOX2 has not yet been examined.

In this study, we hypothesized that normal human epidermal keratinocytes (NHEK) express DUOX proteins, and that their expression is regulated by Th1 or Th2 cytokines. Because it has been demonstrated that the Th2 cytokines, IL-4 and IL-13, play a crucial role in the pathogenesis of atopic dermatitis, as well as in allergic contact dermatitis (12–14), and that they significantly affect keratinocyte functions such as the suppression of gene expression of human β-defensin 3, filaggrin, loricrin, and involucrin (15, 16), we focused on analysis of the effects of Th2 cytokines on the expression of DUOX proteins.

*Department of Dermatology, Tohoku University Graduate School of Medicine, Sendai 980-8574, Japan; †Safety Research, Quality Research Department, POLA Chemical Industries, Totsuka-ku, Yokohama 244-0812, Japan; and ‡Department of Clinical Pharmacy, Tohoku University Graduate School of Pharmaceutical Sciences, Aoba-ku, Sendai 980-8574, Japan

[1]Current address: Shinshu University School of Medicine, Nagano, Japan.

Received for publication March 16, 2010. Accepted for publication February 2, 2011.

This work was supported by the New Energy and Industrial Technology Development Organization, Japan; the Network Medicine Global-COE Program from the Ministry of Education, Culture, Sports, Science and Technology, Japan; and a grant-in-aid for scientific research from the Japan Society for the Promotion of Science (Grant 17790749).

The sequences presented in this article have been submitted to Gene Expression Omnibus under accession number GSE20706 (http://www.ncbi.nlm.nih.gov/geo/query/acc.cgi?acc=GSE20706).

Address correspondence and reprint requests to Dr. Setsuya Aiba, Department of Dermatology, Tohoku University Graduate School of Medicine, 1-1, Seiryo-machi, Aoba-ku, Sendai 980-8574, Japan. E-mail address: saiba@med.tohoku.ac.jp

The online version of this article contains supplemental material.

Abbreviations used in this article: DPI, diphenyleneiodonium; DUOX, dual oxidase; IAA, iodoacetic acid; NHEK, normal human epidermal keratinocytes; NIH, National Institutes of Health; PTP, protein tyrosine phosphatase; ROS, reactive oxygen species; RPLP0, ribosomal protein, large, P0; siRNA, small interfering RNA.

In this study, we first demonstrated using a DNA microarray that, of the seven NOX/DUOX members, IL-4/IL-13 treatment only augments the expression of DUOX1 mRNA. We next confirmed the induction of DUOX1 at the mRNA and protein level by IL-4/IL-13 treatment of NHEK using quantitative real-time PCR and Western blotting, respectively. We further demonstrated that IL-4/IL-13 enhancement of H_2O_2 production depended on their induction of DUOX1 by using small interfering RNA (siRNA) against DUOX1 (DUOX1-siRNA) and diphenyleneiodonium (DPI), an inhibitor of NADPH oxidases.

We next demonstrated, using the DNA microarray, that DUOX1-siRNA suppresses the expression of >50% of the 220 genes that are upregulated by IL-4/IL-13 treatment of NHEK. It is well-known that STAT6 plays an important role in IL-4 and IL-13 signaling (reviewed by Hebenstreit et al. [17]). Therefore, we next demonstrated that STAT6 phosphorylation 24 h after IL-4/IL-13 treatment of NHEK is suppressed by DUOX1-siRNA. Finally, as a possible mechanism by which DUOX1 suppresses STAT6, we showed that oxidation of the catalytic cysteine 215 of protein tyrosine phosphatase (PTP) 1B is regulated by DUOX1 in IL-4/IL-13–treated NHEK. This finding is consistent with the recent establishment of H_2O_2 as an important regulator of eukaryotic signal transduction (reviewed by Veal et al. [18]). These results indicate a role for the DUOX1 that is induced by IL-4/IL-13 treatment of NHEK as a positive regulator of STAT6 signaling.

Materials and Methods

Cell culture and treatment with cytokines

NHEK derived from neonatal foreskin were purchased from Kurabo (Osaka, Japan) and were cultured in serum-free keratinocyte growth medium (HuMedia-KB2; Kurabo) containing 0.15 mM calcium and supplemented with human epidermal growth factor (0.1 ng/ml), insulin (10 μg/ml), hydrocortisone (0.5 μg/ml), gentamicin (50 μg/ml), amphotericin B (50 ng/ml), and bovine brain pituitary extract (0.4% v/v), at 37˚C under 5% CO_2/95% air. The medium was replaced every 2 d. The second-passage NHEK were used for all experiments. When the cells reached ~80% confluence (0 h), they were incubated in the presence or absence of IL-4 (100 ng/ml) and/or IL-13 (100 ng/ml; Peprotec EC, London, U.K.). For intracellular ROS measurement, NHEK were cultured in phenol red-free medium.

RNA isolation

Total RNA was extracted from NHEK using RNeasy Mini Kits according to the manufacturer's instructions (Qiagen, Valencia, CA). The concentration of the obtained total RNA was measured using a Nanodrop spectrophotometer (Thermo Fisher Scientific, Wilmington, DE). RNA quality was determined using the RNA 6000 Nano Kit (Agilent Technologies, Palo Alto, CA) and an Agilent 2100 bioanalyzer (Agilent Technologies), and RNA was stored in RNase-free water at −80˚C. RNA with an RNA integrity number of nine or more was used for further experiments.

Microarray analysis and gene selection criteria

In brief, 500 ng of the total RNA isolated from each sample was amplified and labeled with cyanine-3 using the Quick-Amp Kit (Agilent Technologies). Cyanine-3–labeled cRNA was hybridized to the Whole Human Genome 44K Oligo Microarray (Agilent Technologies) containing 45,015 features representing 41,000 unique probes. The washing and hybridization were carried out according to the manufacturer's instructions. Signals in the scanning image were converted to intensity values using Feature Extraction version 9.5.3. Microarray analyses were repeated three times using different strains of NHEK to identify consistent gene expression changes. The data from all arrays were analyzed using GeneSpring GX10.0.2 software (Agilent Technologies), and global normalization was performed. The normalized data were analyzed to identify genes whose expression was consistently (three of biological replicates) upregulated by an arbitrary cutoff of at least 2-fold after cytokine treatment. Statistical analysis was performed on $\log_2$ expression ratios using a paired Student *t* test. We also performed two-dimensional hierarchical clustering analysis of the genes that were significantly, and at least 2-fold, upregulated by IL-4/IL-13 treatment of NHEK using the Gene Tree and Condition Tree clustering methods within the GeneSpring GX10.0.2 software.

Quantitative real-time RT-PCR

cDNAs were synthesized from 1 μg total RNA extracts in a volume of 20 μl using 0.25 U AMV Reverse Transcriptase XL (TaKaRa Biochemicals, Otsu, Japan) at 42˚C for 45 min in the presence of 50 mM KCl, 10 mM Tris-HCl (pH 8.3), 5 mM $MgCl_2$, 1 mM dNTP, 0.25 U RNase inhibitor, and 0.125 μM of an oligo(dT)-adaptor primer. For each target gene, forward and reverse primers and TaqMan probes were selected using Primer Express 1.0 software, and were prepared by SIGMA GENOSYS (Ishikari, Japan). The forward and reverse primers used for DUOX1 were 5′-CGAGAGGACCATGTGTTGGTT-3′ and 5′-TGCGGGAAAACTTCAGTGG-3′ with the TaqMan probe FAM 5′-TGTGCGGGATTTCTGGCCTGG-3′ TAMRA. The forward and reverse primers used for ribosomal protein, large, P0 (RPLP0) were 5′-CCAGGCGTCCTCGTGG-3′ and 5′-GCGGTGCGTCAGGGATT-3′ with the TaqMan probe FAM 5′-GAGTGACATCGTCTTTAAACCCTGCGTGG-3′ TAMRA. Quantitative real-time RT-PCR amplification mixtures (25 μl) contained 50 ng template cDNA, 5 μM TaqMan probe (0.3 μl), 20 μM forward primers, 20 μM reverse primers (each 0.5 μl), 2 μM reference dye (0.375 μl), and Brilliant II Fast Quantitative PCR Master Mix (12.5 μl) (Stratagene, Santa Clara, CA). Reactions were carried out using the Mx3000p Real-Time Quantitative PCR System (Stratagene). The thermal cycling conditions were 2 min for polymerase activation at 95˚C; then 45 cycles of 95˚C for 5 s and 60˚C for 20 s. Samples were then brought to 4˚C. The levels of cDNA were calculated using standard curves generated with bona fide human cDNAs in which there was a linear relation between the number of cycles required to exceed the threshold and the number of copies of cDNA added. The relative ratio was calculated by dividing the copy number of cDNA for DUOX1 by that of cDNA for RPLP0. RPLP0 was chosen as the endogenous control from a commercially available TaqMan human endogenous control plate (Applied Biosystems), which included 11 candidate controls (data not shown).

Protein extraction and Western blotting

The cells were treated for the indicated time periods with IL-4 and/or IL-13 in HuMedia-KG2 medium. After treatment, the cells were washed twice with cold PBS containing 1 mM pervanadate and were then resuspended in cell lysis buffer containing 0.5 M Tris-HCl pH 7.4, 10% SDS, 20% glycerol, 10% 2-ME, and 0.2% bromophenol blue supplemented with a protease inhibitor mixture (Complete Mini; Roche Diagnostics, Mannheim, Germany). The cells were collected into 1.5-ml centrifuge tubes, vigorously vortexed, and centrifuged at 15,000 × *g* for 5 min at 4˚C. The supernatants containing cell proteins were stored at −80˚C until use. Aliquots of the protein were boiled for 5 min, electrophoresed, and transferred onto polyvinylidene difluoride membranes (Millipore, Bedford, MA). Electroblotted membranes were blocked with 50 mM Tris (pH 7.5) containing 0.1% TBST and 3% nonfat dried milk (Cell Signaling Technology, Beverly, MA) for 1 h at room temperature or, in the case of the anti–phospho-Stat6 Ab, with 5% BSA (Sigma-Aldrich, St. Louis, MO) overnight at 4˚C. The membranes were then incubated overnight at 4˚C with goat anti-human DUOX1 Ab (1:100 dilution; Santa Cruz Biotechnology, Santa Cruz, CA), anti–β-actin mAb (1:100 dilution; Sigma-Aldrich), rabbit anti–phospho-Stat6 Ab (Tyr641) (1:1,000 dilution; Cell Signaling Technology), rabbit anti-Stat6 Ab (1:1,000 dilution; Cell Signaling Technology), or mouse anti-PTP1B Ab (1:200 dilution; BD Biosciences, San Jose, CA) were rinsed with TBST and were then incubated with HRP-conjugated secondary Abs (1:1,000 dilution; Cell Signaling Technology). After additional rinses with TBST, the blots were exposed to LumiGLO reagent (Cell Signaling Technology) and were then visualized using the LAS-1000 (Fujifilm, Tokyo, Japan) according to the manufacturer's instructions. Equal loading was achieved by normalization of the protein concentration using a BCA protein assay (Thermo Scientific, Rockford, IL). Band densities were quantified by using the National Institutes of Health (NIH) ImageJ 1.42 program (NIH, Bethesda, MD).

Measurement of extracellular H_2O_2 and intracellular ROS production

Extracellular H_2O_2 production was measured using the Amplex Red Hydrogen Peroxide/Peroxidase Assay Kit (Molecular Probes, Eugene, OR) (19), according to the manufacturer's protocol. NHEK were incubated in the presence or absence of 100 ng/ml IL-4 and 100 ng/ml IL-13 for 48 h. In some experiments, NHEK were preincubated with 20 μM DPI for 30 min at 37˚C. At the end of the culture, the cells were washed twice with PBS and were then treated with a reaction mixture containing 50 μM Amplex Red reagent and 0.1 U/ml HRP in Krebs-Ringer phosphate buffer glucose (145 mM NaCl, 5.7 mM sodium phosphate, 4.86 mM KCl, 0.54 mM $CaCl_2$, 1.22 mM $MgSO_4$, 5.5 mM glucose, pH 7.35) with or without 5 μM

Table I. Effect of IL-4/IL-13 treatment of NHEK on NOX/DUOX family gene expression assessed by DNA microarray analysis

			Control		IL-4 + IL-13				
Agilent Probe ID	GenBank Accession	Gene Symbol	Mean	SD	Mean	SD	Fold Change	Regulation	*p* Value
A_23_P217280	NM_007052	NOX1	0.004	0.988	1.283	1.787	2.426	Up	0.484
A_23_P316410	NM_013954	NOX1	1.267	1.376	0.001	0.415	2.406	Down	0.169
A_23_P304921	NM_013955	NOX1	0.401	0.986	−0.049	0.421	1.366	Down	0.480
A_23_P217258	NM_000397	NOX2	0.168	0.942	−0.013	0.298	1.134	Down	0.747
A_24_P365767	NM_000397	NOX2	0.374	0.817	−0.102	0.502	1.391	Down	0.380
A_23_P82099	NM_015718	NOX3	0.425	0.987	−0.065	0.371	1.404	Down	0.441
A_24_P739344	NM_016931	NOX4	0.467	0.549	−0.360	0.565	1.773	Down	0.259
A_23_P47148	NM_016931	NOX4	1.429	1.247	−0.162	1.444	3.014	Down	0.128
A_23_P140475	NM_024505	NOX5	0.687	0.517	−0.439	0.442	2.183	Down	0.013
A_23_P54291	NM_017434	DUOX1	−0.016	0.077	1.368	0.397	2.610	Up	0.031
A_24_P316586	AL137592	DUOX1	0.007	0.140	1.152	0.228	2.211	Up	0.012
A_23_P151851	NM_014080	DUOX2	0.631	1.183	0.027	0.547	1.520	Down	0.593
A_24_P35905	NM_014080	DUOX2	0.696	1.132	−0.159	0.636	1.809	Down	0.415

DPI. Amplex Red fluorescence was measured at 37°C for 1 h in a microplate reader (Fluoroskan Ascent; Labsystems, Helsinki, Finland) with the excitation wavelength set at 544 nm and fluorescence detection at 590 nm. In each experiment, the amount of H_2O_2 production was determined using a H_2O_2 standard curve of 0–20 μM, and production was normalized to the protein concentration in the well. The results for each treatment condition represent the means ± SD of triplicate experiments.

Intracellular ROS were measured fluorometrically using the CMH_2DCFDA (Invitrogen Life Technologies) probe according to the manufacturer's protocol. In brief, NHEK were incubated in phenol red-free medium in the presence or absence of 100 ng/ml IL-4 and 100 ng/ml IL-13 for 48 h. The cells were then washed twice with PBS and incubated with 10 μM CM-H_2DCFDA in PBS for 20 min at 37°C in 5% CO_2. The cells were washed twice with PBS and were incubated in Krebs-Ringer phosphate buffer glucose at 37°C for 1 h. NHEK were scanned using a multimode microplate reader Mithras LB940 (Berthold Technologies) with the excitation wavelength set at 485 nm and fluorescence detection at 535 nm. The mean fluorescence intensity was calculated for each treatment and was normalized to the protein concentration in each well. The results for each treatment condition represent the means ± SD of five experiments.

Knockdown of DUOX1 and PTP1B by siRNA

NHEK were seeded onto a 6-well plate at a density of 3×10^5 cells/well to examine mRNA and protein expression, onto a 24-well plate at a density of 1×10^5 cells/well to measure H_2O_2, and onto a 96-well plate at a density of 1×10^4 cells/well to detect intracellular ROS production. Two hours later, the cells were transfected with 10 nM of one of two different siRNA against DUOX1 (DUOX1-siRNA1 and DUOX1-siRNA2), 30 nM siRNA against PTP1B (Stealth siRNA; Invitrogen, Carlsbad, CA) or 10 or 30 nM of a scrambled siRNA using HiPerFect reagent (Qiagen, Tokyo, Japan) according to the manufacturer's protocol. Some cells were treated with only HiPerFect reagent as a mock control. The sequences of the DUOX1-siRNA1 (HSS122734) were UUGGGUAUCUGGCACAUCUGUCACC (sense) and GGUGACAGAUGUGCCAGAUACCCAA (antisense), those of DUOX1-siRNA2 (HSS122735) were UUACAGAACACUUGGCAGCUGACGG (sense) and CCGUCAGCUGCCAAGUGUUCUGUAA (antisense), and those of PTP1B (VHS41290) were UUGAUGUAGUUUAAUCCGACUAUGG (sense) and CCAUAGUCGGAUUAAACUACAUCAA (antisense). Medium GC duplex of stealth RNAi Negative Control Duplexes (Invitrogen) was used as a nonspecific scrambled siRNA. Twenty-four hours after DUOX1-siRNA transfection or 48 h after PTP1B siRNA transfection, NHEK were transferred to growth medium with or without 100 ng/ml IL-4 and 100 ng/ml IL-13.

Detection of PTP1B oxidation

PTP1B oxidation was measured as described previously (20). The buffers used in the following experiments were extensively deoxygenated by bubbling nitrogen gas, and cell lysis was performed in an anaerobic chamber with a continuous flow of nitrogen gas, to avoid spontaneous PTP1B oxidation during cell lysis. After various culture times, the cells were washed with deoxygenated cold PBS and were lysed with deoxygenated lysis buffer containing 50 mM Tris-HCl pH 7.5, 0.5% NP-40, 10% glycerol, and a protease inhibitor mixture (Roche Diagnostics) in the presence or absence of 100 mM iodoacetic acid (IAA; Sigma). IAA alkylates all cysteines except those that are reversibly oxidized. Cell lysates were immunoprecipitated with an anti-PTP1B Ab (BD Biosciences, San Jose, CA) that was immobilized on protein G-Sepharose beads (GE Healthcare, Uppsala, Sweden), and were incubated with 10 mM DTT to reduce the reversibly oxidized cysteine of PTP1B. The precipitates were then irreversibly oxidized to cysteine-sulfonic acid by incubation with 100 μM

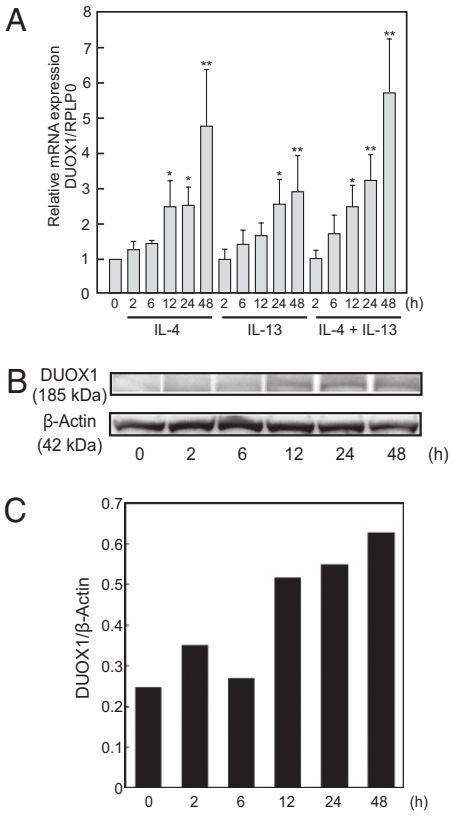

FIGURE 1. Time-dependent expression of DUOX1 mRNA and protein by IL-4 and/or IL-13 treatment of NHEK. *A*, NHEK were treated with 100 ng/ml IL-4 and/or 100 ng/ml IL-13 for the indicated number of hours. DUOX1 mRNA expression was evaluated by quantitative real-time PCR. Data were normalized to that of RPLP0 and are expressed relative to that at 0 h. Data represent the means ± SD of the relative ratio ($n = 3$) from five independent experiments. $^*p < 0.05$, $^{**}p < 0.01$. *B*, NHEK were treated with 100 ng/ml IL-4 and 100 ng/ml IL-13 for the indicated hours. DUOX1 protein expression was evaluated by Western blotting using an anti-DUOX1 Ab. To verify that cell lysates contained equal concentrations of protein, we probed the lysates with anti–β-actin Ab. The results are representative of two independent experiments. *C*, The density of the signals in *B* was measured using NIH image software and the ratio of DUOX1/β-actin expression was calculated.

pervanadate for 1 h at 4°C. The samples were then analyzed by immunoblotting with a monoclonal anti-human/mouse/rat oxidized PTP active site Ab raised against a peptide corresponding to the conserved PTP active site ["(V/I)HCSXG"] in which the catalytic cysteine (C215 in PTP1B) is irreversibly oxidized to cysteine-sulfonic acid (R&D Systems, Minneapolis, MN).

Statistics

The statistical significance of differences in the ratio of DUOX1 mRNA/RPLP0 mRNA between nontreated NHEK (0 h) and cytokine-treated NHEK at the indicated times was examined using Dunnett's test. In cases where multiple groups were compared, data were analyzed using the Tukey–Kramer test. All analyses were conducted using the JMP statistical software version 7.0.1 (SAS Institute, Tokyo, Japan).

Results

Microarray analysis identifies genes whose expression is augmented by IL-4/IL-13 treatment of NHEK

DNA microarray experiments were conducted to examine the effect of IL-4/IL-13 treatment of NHEK on gene expression. These microarrays were used to explore genes that were differentially expressed in three different strains of NHEK that had been treated, or not treated, with 100 ng/ml IL-4 and 100 ng/ml IL-13 for 48 h. After normalization and filtering of signals with low intensity, this analysis indicated that a total of 247 probes (220 genes) were significantly, and at least 2-fold, upregulated in the IL-4/IL-13–treated NHEK compared with nontreated NHEK ($p < 0.05$; paired Student *t* test; Supplemental Table I). All raw microarray data are available at Gene Expression Omnibus (GEO) with the accession number GSE20706 (http://www.ncbi.nlm.nih.gov/geo/query/acc.cgi?acc=GSE20706).

Unsurprisingly, the list of upregulated genes included genes that have already been reported to be upregulated by IL-4 or IL-13 treatment of NHEK or other cells. These genes included: *cathepsin c* (*CTSC*) (21), *hydroxy-δ-5-steroid dehydrogenase, 3 β- and steroid δ-isomerase 1* (*HSD3B1*) (22), *tenascin C* (*TNC*) (23), *serpin peptidase inhibitor, clade B* (*OVA*), *member 3* (*SERPINB3*), *serpin peptidase inhibitor, clade B* (*OVA*), *member 4* (*SERPINB4*) (24), *chemokine (C-C motif) ligand 26* (*CCL26*) (25), *chemokine (C-X-C motif) ligand 16* (*CXCL16*) (26), *hydroxy-δ-5-steroid dehydrogenase, 3 β- and steroid δ-isomerase 2* (*HSD3B2*) (22), *carbonic anhydrase II* (*CA2*) (27), and *hyaluronan synthase 3* (*HAS3*) (28). To validate these microarray data, we examined the induction of mRNA for *CTSC*, *CA2*, *SERPINB3*, *HSD3B1*, and *TNC* after 48-h treatment with 100 ng/ml IL-4 and 100 ng/ml IL-13 using quantitative real-time PCR (Supplemental Fig. 1). These results confirmed the microarray data and supported the validity of our DNA microarray analysis.

DUOX1 expression is upregulated by NHEK treatment with IL-4 and/or IL-13

We next focused our microarray analysis on the effect of IL-4 and IL-13 treatment on the mRNA expression of the seven NOX/DUOX family members. The summarized data shown in Table I clearly indicated that, of these seven family members, only DUOX1 mRNA was significantly augmented by treatment with IL-4/IL-13. To confirm the augmented expression of DUOX1 mRNA by IL-4/IL-13 treatment, we next performed quantitative real-time PCR analysis of DUOX1 mRNA expression using mRNA isolated from NHEK treated with 100 ng/ml IL-4 and/or 100 ng/ml IL-13 for 0, 2, 6, 12, 24, or 48 h (Fig. 1*A*), or from NHEK treated with different concentrations of IL-4 and/or IL-13 for 48 h (Supplemental Fig. 2). The results clearly demonstrated that IL-4, IL-13, and combined IL-4/IL-13 treatment augmented DUOX1 mRNA expression by NHEK in a time- and dose-dependent manner. Compared with the nontreated control, NHEK treated with 100 ng/ml IL-4 or IL-4/IL-13 for 12, 24, or 48 h, with 100 ng/ml IL-13 for 24 or 48 h, with >10 ng/ml IL-4 or IL-4/IL-13 for 48 h, or with >30 ng/ml IL-13 for 48 h significantly increased DUOX1 mRNA expression ($p < 0.05$). Furthermore, we confirmed that DUOX1 mRNA expression was not dependent on the calcium concentration in the culture medium (Supplemental Fig. 3). To confirm that expression of NOX/DUOX family members other than DUOX1 was not induced by IL-4/IL-13 treatment, we examined their mRNA expression by PCR using the primers described in Supplemental Table IV. This result indicated that, although NOX2, NOX4, NOX5, NOX5L, DUOX1, and DUOX2 were expressed at basal level, none of them was upregulated by IL-4/IL-13 treatment (Supplemental Fig. 4).

We next examined the augmented expression of DUOX1 by IL-4/IL-13 treatment of NHEK at the protein level by Western blotting with an anti-DUOX1 Ab. As expected, DUOX1 protein expression was also induced at 12 h after IL-4/IL-13 treatment (Fig. 1*B*, 1*C*). The cell lysates were also probed with anti–β-actin Ab (42 kDa) to verify that the cell lysates contained equal concentrations of protein.

IL-4/IL-13 treatment of NHEK increases extracellular H_2O_2 and intracellular ROS production in a DUOX1-dependent manner

Because it has been reported that DUOX proteins produce H_2O_2 in respiratory tract epithelial cells (4–7), we next examined whether IL-4 and/or IL-13 treatment of NHEK increases extracellular H_2O_2 production. Because treatment of NHEK with IL-4/IL-13 augments the expression of DUOX1 mRNA and protein in a time-dependent manner, we measured extracellular H_2O_2 production in NHEK 48 h after IL-4 and/or IL-13 treatment using a highly sensitive and quantitative fluorescence microplate assay of H_2O_2 that uses an HRP substrate *N*-acetyl-3,7-dihydroxyphenoxazine (19) (Fig. 2). To clarify the involvement of NOX/DUOX family members in IL-4– and/or IL-13–induced extracellular H_2O_2 pro-

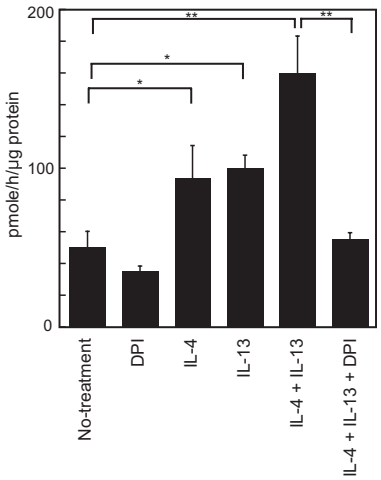

FIGURE 2. IL-4 and/or IL-13 augment the production of extracellular H_2O_2 by NHEK. NHEK were treated with or without the indicated combinations of 100 ng/ml IL-4, 100 ng/ml IL-13, and DPI for 48 h, after which extracellular H_2O_2 production was determined by using the Amplex Red Hydrogen Peroxide/Peroxidase Assay Kit. The level of H_2O_2 production was determined for each experiment using a H_2O_2 standard curve, and levels were normalized using the protein content of each well. Data are presented as means ± SD ($n = 6$) and are representative of five independent experiments. $^{**}p < 0.01$.

duction, the effect of DPI, an inhibitor of NADPH oxidase (29), on H_2O_2 production was assayed. The results clearly showed that NHEK treated with IL-4 and/or IL-13 for 48 h significantly increased extracellular H_2O_2 production, which was completely abrogated by treatment with DPI. These data suggest that NOX/DUOX family enzymes were involved in this process.

Next, we determined whether extracellular H_2O_2 production that was augmented by IL-4/IL-13 treatment of NHEK depended on DUOX1 expression by using siRNA against DUOX1 (DUOX1-siRNA). Two different DUOX1-siRNAs, DUOX1-siRNA1 and DUOX1-siRNA2, were designed for this purpose, as well as a scrambled siRNA that was used as a control. Before examination of the effects of these DUOX1-siRNAs on extracellular H_2O_2 production, we first verified their efficacy by analysis of their effect on cellular DUOX1 mRNA and protein levels using quantitative real-time PCR and Western blotting, respectively. DUOX1-siRNA1 and DUOX1-siRNA2 decreased the DUOX1 mRNA level in IL-4/IL-13–stimulated NHEK by 90 and 80%, respectively, 72 h after transfection, whereas a scrambled siRNA, or mock transfection did not affect its level (Fig. 3*A*). DUOX1-siRNA1, but not the scrambled siRNA, also suppressed DUOX1 protein expression (Fig. 3*B*, 3*C*). We also examined the effects of DUOX1-siRNA1 24 and 48 h after transfection and found that it could suppress DUOX1 mRNA expression even 48 h after transfection (Supplemental Fig. 5).

Using these DUOX1-siRNAs, we demonstrated that NHEK, whose DUOX1 mRNA expression was knocked down by transfection of either DUOX1-siRNA1 or DUOX1-siRNA2, showed a significantly decreased H_2O_2 production in response to IL-4/IL-13, compared with cells without transfection or transfected with control siRNA (Fig. 3*D*). In addition, we examined whether IL-4/IL-13 treatment also induced intracellular ROS production and, if so, whether this was dependent on DUOX1 expression. Measurement of intracellular ROS using the CMH_2DCFDA probe clearly showed that IL-4/IL-13 treatment induced intracellular ROS production, which was mediated by IL-4/IL-13–induced DUOX1 expression (Fig. 3*E*). Collectively, these results suggest that the augmented extracellular H_2O_2 and intracellular ROS production induced by IL-4/IL-13 treatment of NHEK were mediated by the induced DUOX1.

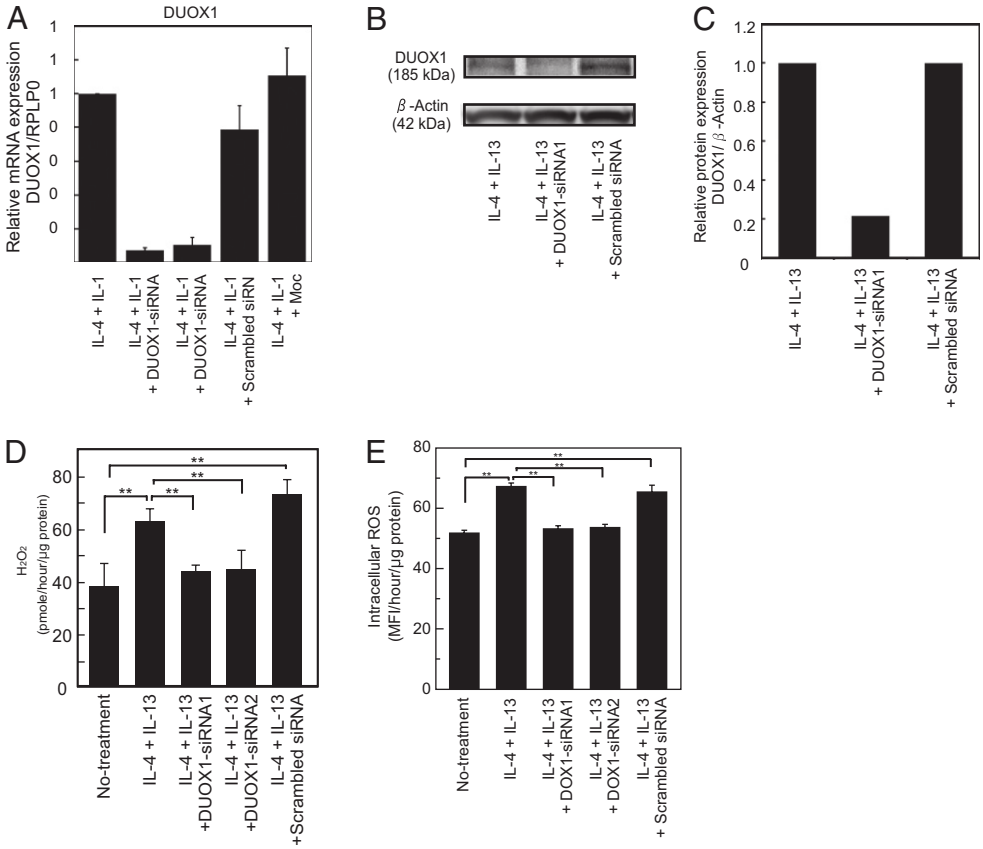

FIGURE 3. DUOX1-siRNA knockdown suppresses extracellular H_2O_2 production by IL-4/IL-13–treated NHEK. NHEK were transfected with 10 nM of one of two different siRNA sequences against DUOX1 (DUOX1-siRNA1 and DUOX1-siRNA2) or with 10 nM of a scrambled siRNA using the HiPerFect reagent. The indicated NHEK were treated only with HiPerFect reagent as a mock control. At 24 h after transfection, NHEK were transferred to growth medium in the presence or absence of IL-4/IL-13, and were incubated for 48 h. *A*, DUOX1 mRNA expression was examined by quantitative real-time PCR, and values were normalized to that of RPLP0. All values are expressed relative to values of nontransfected cells treated with IL-4/IL-13, which were assigned a value of 1. Data are presented as the means ± SD of the relative ratio ($n = 3$) from three independent experiments. $^{**}p < 0.01$. *B*, DUOX1 protein expression was evaluated by Western blotting using an anti-DUOX1 Ab. To verify that cell lysates contained equal concentrations of protein, we also probed the lysates with anti–β-actin Ab. The results are representative of three independent experiments. *C*, The densities of the signals in *B* were measured using NIH image software and are representative of three different experiments. In addition, NHEK were treated or not with IL-4/IL-13 for 48 h. The indicated IL-4/IL-13–treated NHEK were transfected with either DUOX1-siRNA1, DUOX1-siRNA2, or scrambled siRNA 24 h before IL-4/IL-13 treatment. *D*, Extracellular H_2O_2 production (pmol/h/μg protein) was determined as described in *Materials and Methods*. Data are presented as means ± SD ($n = 6$) and are representative of two independent experiments. $^{**}p < 0.01$. *E*, Intracellular ROS was determined using the CM-H_2DCFDA probe. The level of intracellular ROS was normalized using the protein content of each well. Data are presented as means ± SD ($n = 5$) and are representative of two independent experiments. $^{**}p < 0.01$.

DUOX1-siRNA suppresses the augmented expression of >50% of the genes upregulated by IL-4/IL-13 treatment of NHEK

It has recently been shown that H_2O_2 plays important roles as a signaling molecule in the regulation of a variety of biological processes (18). Therefore, to identify the possible role of the augmented DUOX1 expression induced by IL-4/IL-13 treatment of NHEK in cell signaling related to gene expression, we investigated the effect of DUOX1-siRNA on the gene expression profile of IL-4/IL-13–treated NHEK using the DNA microarray. We also performed two-dimensional hierarchical clustering analysis of the genes that were significantly, and at least 2-fold, upregulated by IL-4/IL-13 treatment of NHEK (Fig. 4*A*). Similarities in the gene expression pattern among different treatments are represented as a "condition tree" on the top of the matrix. The condition tree clearly demonstrated that the genes expressed after IL-4/IL-13 treatment of NHEK transfected with DUOX1-siRNA were clustered with the genes of nontreated cells, whereas the genes induced by IL-4/IL-13 treatment in the absence of DUOX1-siRNA were clustered on a separate branch.

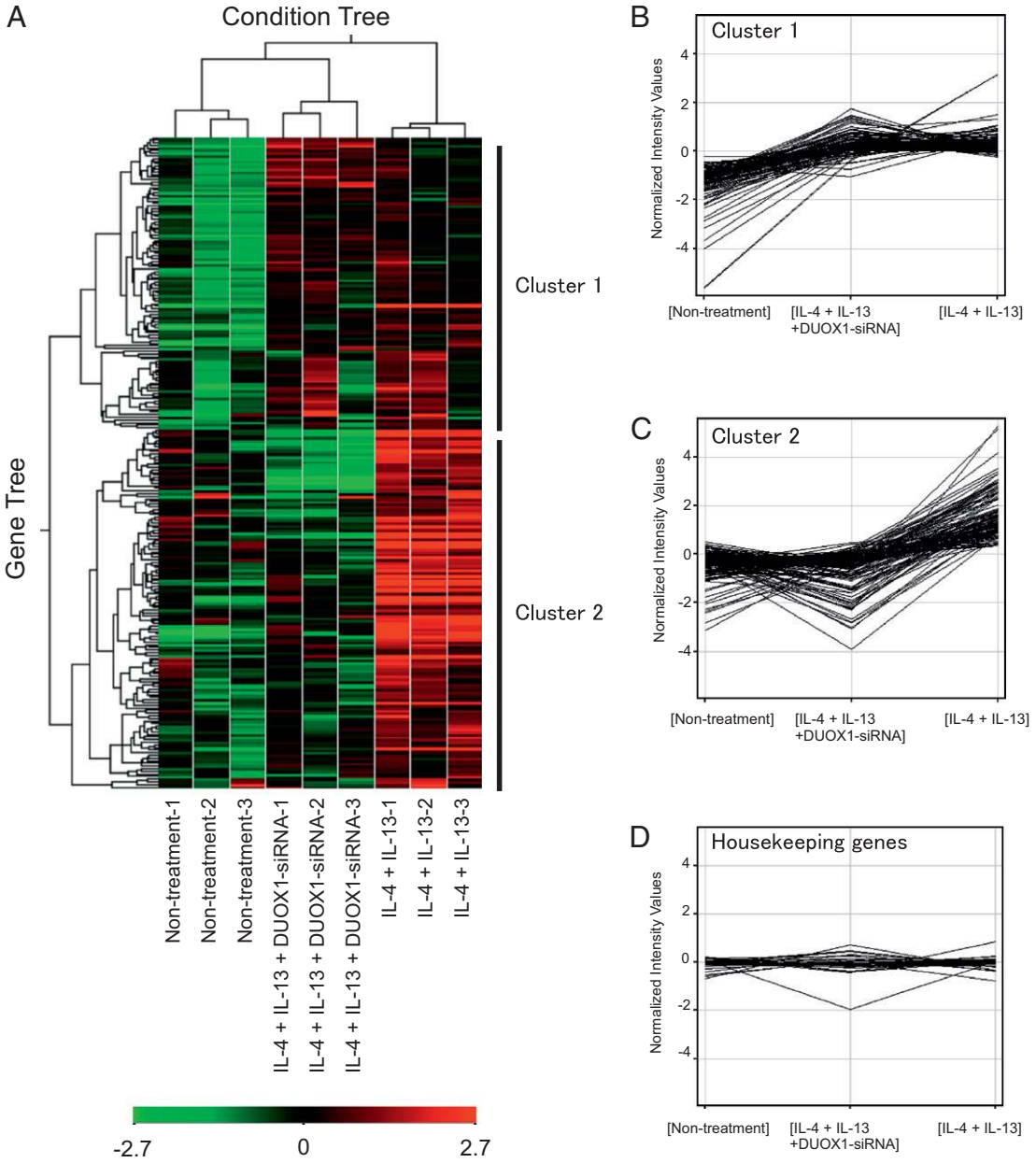

FIGURE 4. Two-dimensional hierarchical clustering analysis of genes whose expression was augmented by IL-4/IL-13 treatment of NHEK. NHEK were treated with IL-4/IL-13 for 48 h. The indicated NHEK were transfected with DUOX1-siRNA 24 h before treatment with IL-4/IL-13. After treatment, RNA was isolated from NHEK and was examined using a DNA microarray. *A*, Two-dimensional hierarchical clustering analysis was performed on the data of the gene-expression profiles of the 247 probes (220 genes) that were upregulated by IL-4/IL-13. The distances between the nine samples are shown. Each row and column represents a gene and a single experimental sample, that is, nontreatment, IL-4/IL-13 treatment, or IL-4/IL-13 treatment with DUOX1-siRNA transfection. The colored bars indicate upregulated genes (red), downregulated genes (green), and genes whose expression was similar to that of the nontreated control (black). The Gene Tree and the Condition Tree show the similarities in the expression pattern among genes and experiments, respectively. *B* and *C*, Of the 247 probes (220 genes) that were upregulated by IL-4/IL-13, genes whose expression was not affected (*B*, cluster 1) or whose expression was suppressed (*C*, cluster 2) were selected and changes in the normalized intensity values are shown. *D*, Changes in the normalized intensity values for 13 housekeeping genes (23 probes) are indicated.

The dendrogram on the left side of this matrix represents similarities in gene expression patterns as a "gene tree." A total of 247 probes (220 genes) were clustered into 2 large clusters, clusters 1 and 2. Cluster 1 included the IL-4/IL-13–induced genes whose expression was not affected by DUOX1-siRNA (Fig. 4*B*, Supplemental Table II), whereas cluster 2 included the IL-4/IL-13–induced genes whose expression was dramatically suppressed by DUOX1-siRNA (Fig. 4*C*). In contrast, analysis of 13 human housekeeping genes (23 probes) (*ACTB*, *ATP5F1*, *B2M*, *GAPDH*, *GUSB*, *HPRT1*, *PGK1*, *PPIA*, *RPLP0*, *RPS18*, *TBP*, *TFR2*, *YWHAZ*) that have been reported to be unaffected by alteration of experimental conditions indicated that these genes except for GAPDH did not show a 2-fold or greater change after IL-4/IL-13 treatment of cells transfected with DUOX1-siRNA (Fig. 4*D*). These data suggest that the DUOX-1 siRNA that we used for our experiments only affected the expression of specific NHEK genes.

Unexpectedly, >50% of the IL-4/IL-13–induced genes, that is, 137 probes (119 genes), were in cluster 2 (Supplemental Table III), which suggests the possibility that DUOX1 regulates the main signaling pathway of IL-4/IL-13 signaling. In considering how DUOX1 might regulate IL-4/IL-13 induction of gene expression, we noted that the function of the transcription factor STAT6 is known to be tightly connected to IL-4 and IL-13 signaling [reviewed by Hebenstreit et al. (17)]. Indeed, cluster 2 genes included the CCL26 gene whose expression is known to be augmented via STAT6 activation after IL-4/IL-13 stimulation (25). We therefore speculated that DUOX1 expression induced by IL-4/IL-13 treatment of NHEK might regulate STAT6 activation.

DUOX1-siRNA suppresses the phosphorylation of STAT6 and oxidative inactivation of PTP1B

STAT6 is regulated by phosphorylation. It has also been recently demonstrated that ROS play an important role in facilitating signal transduction by transient inhibition of the catalytic activity of PTPs (30, 31). We therefore speculated that DUOX1 might influence STAT6 function by regulation of STAT6 phosphorylation via DUOX1 modulation of phosphatase activity. To test this possibility, we first analyzed the effect of transfection of DUOX1-siRNA on STAT6 phosphorylation induced by IL-4/IL-13 treatment of NHEK. Consistent with the efficient knockdown of DUOX1 48 h after siRNA transfection (Supplemental Fig. 5), DUOX1-siRNA suppressed phosphorylation of STAT6 24 h after IL-4/IL-13 stimulation. STAT6 phosphorylation was not significantly suppressed at any time point in either nontransfected NHEK or in NHEK transfected with a scrambled siRNA (Fig. 5*A*, 5*B*). This result suggests that DUOX1 is important for the late phase of STAT6 phosphorylation induced by IL-4/IL-13 treatment of NHEK at 24 h after treatment.

Of the known PTPs, PTP1B has been reported to be a nonredundant negative regulator of IL-4– or IL-13–induced STAT6 signaling in hematopoietic and nonhematopoietic cells (20, 32). Therefore, to determine whether the DUOX1 modulation of STAT6 induced by IL-4/IL-13 treatment of NHEK might be mediated by DUOX1-induced oxidative inactivation of PTP1B, we assayed the effect of DUOX1-siRNA transfection on the time-dependent oxidation of PTP1B in IL-4/IL-13–treated NHEK. Oxidation of PTP1B was analyzed after lysis of the cells in the presence or absence of the alkylating agent IAA, at different time points after IL-4/IL-13 treatment. IAA alkylates all cysteines except those that are reversibly oxidized. PTP1B was then immunoprecipitated, reduced with DTT, irreversibly oxidized with pervanadate, and analyzed by Western blotting with an mAb against the oxidized PTP-active site (33). In these experiments, this Ab detected only reversibly oxidized PTP1B in the presence

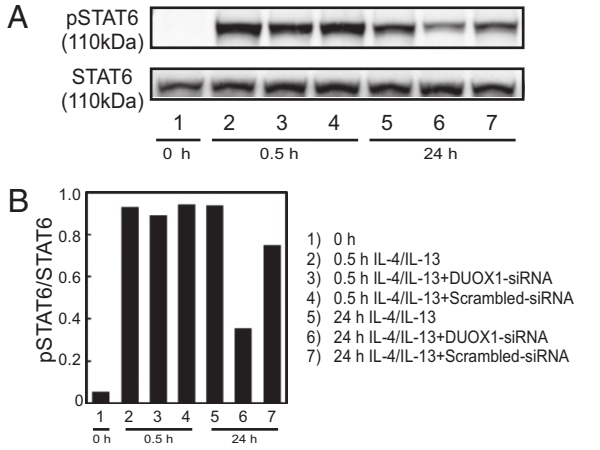

FIGURE 5. DUOX1-siRNA suppresses the phosphorylation of STAT6 in NHEK at 24 h after IL-4/IL-13 treatment. *A*, NHEK were transfected with 10 nM DUOX1-siRNA1 (*lanes 3*, *6*) or with 10 nM of a scrambled siRNA (*lanes 4*, *7*) using the HiPerFect reagent, or not transfected (*lanes 1*, *2*, *5*). At 24 h after transfection, NHEK were transferred to growth medium and were treated with IL-4/IL-13 at the indicated times. Total cell lysates were separated by SDS-PAGE, and the phosphorylation of STAT6 was evaluated by Western blotting using an anti–phospho-Stat6 (Tyr641) Ab. To verify that cell lysates contained equal concentrations of STAT6 protein, we also probed the lysates with an anti-STAT6 Ab. Data are representative of three independent experiments. *B*, The densities of the signals in *A* were measured using NIH image software.

of IAA, whereas it reacted with all PTP1B in the absence of IAA. These results showed that transfection of DUOX1-siRNA, but not scrambled siRNA, significantly suppressed PTP1B oxidation at 24 h after IL-4/IL-13 treatment (Fig. 6*A*, 6*B*), which suggests that the

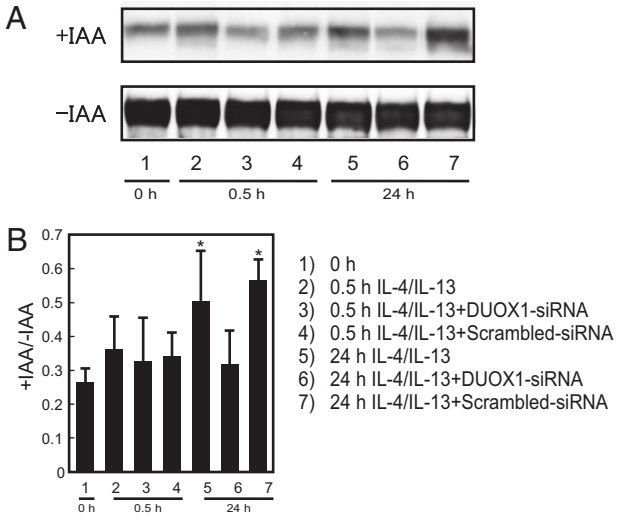

FIGURE 6. DUOX1-siRNA suppresses the oxidation of PTP1B in NHEK at 24 h after IL-4/IL-13 treatment. *A*, NHEK were transfected with 10 nM DUOX1-siRNA1 (*lanes 3*, *6*) or with 10 nM of a scrambled siRNA (*lanes 4*, *7*) using the HiPerFect reagent, or were not transfected (*lanes 1*, *2*, *5*). At 24 h after transfection, NHEK were transferred to growth medium and were treated with IL-4/IL-13 for the indicated times. Cell lysates were prepared in the presence (*upper panel*) or absence (*lower panel*) of IAA and were immunoprecipitated with an anti-PTP1B Ab. The immune complexes were then treated with DTT followed by pervanadate before immunoblotting using a mAb that recognizes oxidized PTP1B. *B*, We conducted three independent experiments and measured the densities of the signals using NIH image software. The summarized data are shown with statistical significance ($n = 3$). *$p < 0.05$.

STAT6 phosphorylation induced at 24 h after IL-4/IL-13 treatment of NHEK was at least partly caused by oxidative inactivation of PTP1B by DUOX1.

PTP1B-siRNA promotes the phosphorylation of STAT6

To further clarify the causative relation between the activity of PTP1B and STAT6 phosphorylation, we examined the effects of PTP1B-specific siRNA on STAT6 phosphorylation by Western blotting. As expected, PTP1B-specific siRNA, which suppressed PTP1B expression 72 h after transfection (Supplemental Fig. 6*A*, 6*B*), augmented STAT6 phosphorylation (Supplemental Fig. 6*C*, 6*D*) compared with a scrambled siRNA.

Discussion

This study is the first demonstration, to our knowledge, that treatment of NHEK with IL-4 and/or IL-13 augments the expression of DUOX1 mRNA and protein in a time- and dose-dependent manner and increases their extracellular H_2O_2 and intracellular ROS production. Furthermore, our studies using DPI or DUOX1-siRNA indicated that the increased H_2O_2 production and intracellular ROS were mostly caused by IL-4/IL-13–induced DUOX1 expression. Although several articles show that DUOX proteins are expressed in respiratory tract epithelial cells and are novel H_2O_2 cellular sources (4–7), to our knowledge, the expression of DUOX1 or DUOX2 has not been reported in epidermal keratinocytes. However, our studies are consistent with those of Harper et al. (8), who reported that IL-4/IL-13 induces DUOX1 mRNA expression in respiratory tract epithelium.

We have also demonstrated a potential pathway through which DUOX1 might influence NHEK signaling. Although DUOX1 is known to play a role in supplying H_2O_2 to thyroperoxidase and lactoperoxidase in thyroid and nonthyroid tissues, respectively (34), it was unlikely that DUOX1 plays either of these roles in NHEK, because Vyas et al. (35) have clearly demonstrated the lack of thyroperoxidase or lactoperoxidase in NHEK.

In this study, we found that DUOX1 regulates the expression of >50% of the genes induced by IL-4/IL-13 treatment by using a combination of DNA microarray analysis and DUOX siRNA knockdown. These analyses suggested that DUOX1 might regulate the activity of a transcription factor, and indeed, we demonstrated that DUOX1 induced by IL-4/IL-13 treatment of NHEK augments STAT6 phosphorylation. It has been previously demonstrated that STAT1 activation by macrophages, immediately after ligand-induced activation of the signal regulatory protein α, is dependent on H_2O_2 produced by some pre-existing NOX proteins (36). In addition, Sharma et al. (20) have recently reported that, immediately after ligand-dependent activation, the IL-4R generates ROS via PI3K-dependent activation of NOX1 and NOX5L. ROS, in turn, promotes IL-4R activation by oxidatively inactivating PTP1B that is physically associated with, and deactivates, the IL-4R.

However, to the best of our knowledge, our study is the first report that NOX/DUOX family proteins induced by ligand stimulation can increase the magnitude and duration of STAT signaling. Recently, Harper et al. (8) have shown that a Th1 cytokine induces the expression of DUOX2 leading to H_2O_2 production in respiratory tract epithelial cells, whereas Th2 cytokines induce the expression of DUOX1. Similarly, Si et al. (37) have shown that platelet-activating factor-induced STAT5 increases the expression of NOX5-S with augmented production of H_2O_2. Although these studies did not clarify the role of H_2O_2 in STAT signal transduction, our study suggests the possibility that these induced NOX/DUOX family proteins also positively regulate STAT signaling.

We have also shown that DUOX1 induced by IL-4/IL-13 oxidizes the catalytic cysteine of the PTP active site of PTP1B. This finding is consistent with the literature that NOX-DUOX–derived ROS regulates cell function through redox-sensitive cysteine residues. This type of regulation has been most convincingly demonstrated for PTPs (38–40). These results, that DUOX1 modulates oxidative inactivation of PTP1B, therefore reveal a novel role of epidermal DUOX1 expression in creating a positive feedback loop for IL-4/IL-13 signaling in NHEK. In our study, we demonstrated the active role of PTP1B in this feedback mechanism by using PTP1B siRNA.

Finally, Sharma et al. (20) have demonstrated that oxidative inactivation of PTP1B by other cytokine-generated ROS such as that generated by TNF-α can amplify activation of the IL-4R in the same cell. Similarly, this study highlights the role of ROS in the regulation of the duration of STAT6 activation after IL-4/IL-13 treatment of keratinocytes. It is well-known that the Th2 cytokines, IL-4 and IL-13, play a crucial role in the pathogenesis of atopic dermatitis, as well as in ACD (12–14). In addition to IL-4 and IL-13, TNF-α has also been suggested to play some role in the pathogenesis of these disorders (41–43). Therefore, it is conceivable that ROS generated by TNF-α and Th2 cytokines may synergistically stimulate epidermal STAT6 signaling via upregulation of NOX/DUOX family members in these inflammatory skin disorders.

Acknowledgments

We thank Yumiko Ito for technical assistance.

Disclosures

The authors have no financial conflicts of interest.

References

1. Bedard, K., and K. H. Krause. 2007. The NOX family of ROS-generating NADPH oxidases: physiology and pathophysiology. *Physiol. Rev.* 87: 245–313.
2. Lambeth, J. D. 2004. NOX enzymes and the biology of reactive oxygen. *Nat. Rev. Immunol.* 4: 181–189.
3. Lambeth, J. D. 2002. Nox/Duox family of nicotinamide adenine dinucleotide (phosphate) oxidases. *Curr. Opin. Hematol.* 9: 11–17.
4. Geiszt, M., J. Witta, J. Baffi, K. Lekstrom, and T. L. Leto. 2003. Dual oxidases represent novel hydrogen peroxide sources supporting mucosal surface host defense. *FASEB J.* 17: 1502–1504.
5. Forteza, R., M. Salathe, F. Miot, R. Forteza, and G. E. Conner. 2005. Regulated hydrogen peroxide production by Duox in human airway epithelial cells. *Am. J. Respir. Cell Mol. Biol.* 32: 462–469.
6. Shao, M. X., and J. A. Nadel. 2005. Dual oxidase 1-dependent MUC5AC mucin expression in cultured human airway epithelial cells. *Proc. Natl. Acad. Sci. USA* 102: 767–772.
7. Schwarzer, C., T. E. Machen, B. Illek, and H. Fischer. 2004. NADPH oxidase-dependent acid production in airway epithelial cells. *J. Biol. Chem.* 279: 36454–36461.
8. Harper, R. W., C. Xu, J. P. Eiserich, Y. Chen, C. Y. Kao, P. Thai, H. Setiadi, and R. Wu. 2005. Differential regulation of dual NADPH oxidases/peroxidases, Duox1 and Duox2, by Th1 and Th2 cytokines in respiratory tract epithelium. *FEBS Lett.* 579: 4911–4917.
9. Chamulitrat, W., W. Stremmel, T. Kawahara, K. Rokutan, H. Fujii, K. Wingler, H. H. Schmidt, and R. Schmidt. 2004. A constitutive NADPH oxidase-like system containing gp91phox homologs in human keratinocytes. *J. Invest. Dermatol.* 122: 1000–1009.
10. Valencia, A., and I. E. Kochevar. 2008. Nox1-based NADPH oxidase is the major source of UVA-induced reactive oxygen species in human keratinocytes. *J. Invest. Dermatol.* 128: 214–222.
11. He, Y. Y., J. L. Huang, M. L. Block, J. S. Hong, and C. F. Chignell. 2005. Role of phagocyte oxidase in UVA-induced oxidative stress and apoptosis in keratinocytes. *J. Invest. Dermatol.* 125: 560–566.
12. Hamid, Q., M. Boguniewicz, and D. Y. Leung. 1994. Differential in situ cytokine gene expression in acute versus chronic atopic dermatitis. *J. Clin. Invest.* 94: 870–876.
13. Homey, B., M. Steinhoff, T. Ruzicka, and D. Y. Leung. 2006. Cytokines and chemokines orchestrate atopic skin inflammation. *J. Allergy Clin. Immunol.* 118: 178–189.
14. Neis, M. M., B. Peters, A. Dreuw, J. Wenzel, T. Bieber, C. Mauch, T. Krieg, S. Stanzel, P. C. Heinrich, H. F. Merk, et al. 2006. Enhanced expression levels of

IL-31 correlate with IL-4 and IL-13 in atopic and allergic contact dermatitis. *J. Allergy Clin. Immunol.* 118: 930–937.
15. Howell, M. D., B. E. Kim, P. Gao, A. V. Grant, M. Boguniewicz, A. Debenedetto, L. Schneider, L. A. Beck, K. C. Barnes, and D. Y. Leung. 2007. Cytokine modulation of atopic dermatitis filaggrin skin expression. *J. Allergy Clin. Immunol.* 120: 150–155.
16. Kim, B. E., D. Y. Leung, M. Boguniewicz, and M. D. Howell. 2008. Loricrin and involucrin expression is down-regulated by Th2 cytokines through STAT-6. *Clin. Immunol.* 126: 332–337.
17. Hebenstreit, D., G. Wirnsberger, J. Horejs-Hoeck, and A. Duschl. 2006. Signaling mechanisms, interaction partners, and target genes of STAT6. *Cytokine Growth Factor Rev.* 17: 173–188.
18. Veal, E. A., A. M. Day, and B. A. Morgan. 2007. Hydrogen peroxide sensing and signaling. *Mol. Cell* 26: 1–14.
19. Mohanty, J. G., J. S. Jaffe, E. S. Schulman, and D. G. Raible. 1997. A highly sensitive fluorescent micro-assay of H2O2 release from activated human leukocytes using a dihydroxyphenoxazine derivative. *J. Immunol. Methods* 202: 133–141.
20. Sharma, P., R. Chakraborty, L. Wang, B. Min, M. L. Tremblay, T. Kawahara, J. D. Lambeth, and S. J. Haque. 2008. Redox regulation of interleukin-4 signaling. *Immunity* 29: 551–564.
21. Matsui, K., N. Yuyama, M. Akaiwa, N. L. Yoshida, M. Maeda, Y. Sugita, and K. Izuhara. 2002. Identification of an alternative splicing variant of cathepsin C/dipeptidyl-peptidase I. *Gene* 293: 1–7.
22. Simard, J., M. L. Ricketts, S. Gingras, P. Soucy, F. A. Feltus, and M. H. Melner. 2005. Molecular biology of the 3beta-hydroxysteroid dehydrogenase/delta5-delta4 isomerase gene family. *Endocr. Rev.* 26: 525–582.
23. Ogawa, K., M. Ito, K. Takeuchi, A. Nakada, M. Heishi, H. Suto, K. Mitsuishi, Y. Sugita, H. Ogawa, and C. Ra. 2005. Tenascin-C is upregulated in the skin lesions of patients with atopic dermatitis. *J. Dermatol. Sci.* 40: 35–41.
24. Mitsuishi, K., T. Nakamura, Y. Sakata, N. Yuyama, K. Arima, Y. Sugita, H. Suto, K. Izuhara, and H. Ogawa. 2005. The squamous cell carcinoma antigens as relevant biomarkers of atopic dermatitis. *Clin. Exp. Allergy* 35: 1327–1333.
25. Kagami, S., H. Saeki, M. Komine, T. Kakinuma, Y. Tsunemi, K. Nakamura, K. Sasaki, A. Asahina, and K. Tamaki. 2005. Interleukin-4 and interleukin-13 enhance CCL26 production in a human keratinocyte cell line, HaCaT cells. *Clin. Exp. Immunol.* 141: 459–466.
26. Day, C., R. Patel, C. Guillen, and A. J. Wardlaw. 2009. The chemokine CXCL16 is highly and constitutively expressed by human bronchial epithelial cells. *Exp. Lung Res.* 35: 272–283.
27. Kamsteeg, M., P. L. Zeeuwen, G. J. de Jongh, D. Rodijk-Olthuis, M. E. Zeeuwen-Franssen, P. E. van Erp, and J. Schalkwijk. 2007. Increased expression of carbonic anhydrase II (CA II) in lesional skin of atopic dermatitis: regulation by Th2 cytokines. *J. Invest. Dermatol.* 127: 1786–1789.
28. Ohtani, T., A. Memezawa, R. Okuyama, T. Sayo, Y. Sugiyama, S. Inoue, and S. Aiba. 2009. Increased hyaluronan production and decreased E-cadherin expression by cytokine-stimulated keratinocytes lead to spongiosis formation. *J. Invest. Dermatol.* 129: 1412–1420.
29. Riganti, C., E. Gazzano, M. Polimeni, C. Costamagna, A. Bosia, and D. Ghigo. 2004. Diphenyleneiodonium inhibits the cell redox metabolism and induces oxidative stress. *J. Biol. Chem.* 279: 47726–47731.
30. Rhee, S. G., Y. S. Bae, S. R. Lee, and J. Kwon. 2000. Hydrogen peroxide: a key messenger that modulates protein phosphorylation through cysteine oxidation. *Sci. STKE* 2000: pe1.
31. Tonks, N. K. 2006. Protein tyrosine phosphatases: from genes, to function, to disease. *Nat. Rev. Mol. Cell Biol.* 7: 833–846.
32. Lu, X., R. Malumbres, B. Shields, X. Jiang, K. A. Sarosiek, Y. Natkunam, T. Tiganis, and I. S. Lossos. 2008. PTP1B is a negative regulator of interleukin 4-induced STAT6 signaling. *Blood* 112: 4098–4108.
33. Persson, C., T. Sjöblom, A. Groen, K. Kappert, U. Engström, U. Hellman, C. H. Heldin, J. den Hertog, and A. Ostman. 2004. Preferential oxidation of the second phosphatase domain of receptor-like PTP-alpha revealed by an antibody against oxidized protein tyrosine phosphatases. *Proc. Natl. Acad. Sci. USA* 101: 1886–1891.
34. Geiszt, M., and T. L. Leto. 2004. The Nox family of NAD(P)H oxidases: host defense and beyond. *J. Biol. Chem.* 279: 51715–51718.
35. Vyas, P. M., S. Roychowdhury, S. B. Koukouritaki, R. N. Hines, S. K. Krueger, D. E. Williams, W. M. Nauseef, and C. K. Svensson. 2006. Enzyme-mediated protein haptenation of dapsone and sulfamethoxazole in human keratinocytes: II. Expression and role of flavin-containing monooxygenases and peroxidases. *J. Pharmacol. Exp. Ther.* 319: 497–505.
36. Alblas, J., H. Honing, C. R. de Lavalette, M. H. Brown, C. D. Dijkstra, and T. K. van den Berg. 2005. Signal regulatory protein alpha ligation induces macrophage nitric oxide production through JAK/STAT- and phosphatidylinositol 3-kinase/Rac1/NAPDH oxidase/H2O2-dependent pathways. *Mol. Cell. Biol.* 25: 7181–7192.
37. Si, J., J. Behar, J. Wands, D. G. Beer, D. Lambeth, Y. E. Chin, and W. Cao. 2008. STAT5 mediates PAF-induced NADPH oxidase NOX5-S expression in Barrett's esophageal adenocarcinoma cells. *Am. J. Physiol. Gastrointest. Liver Physiol.* 294: G174–G183.
38. Hunter, T. 2000. Signaling—2000 and beyond. *Cell* 100: 113–127.
39. Barford, D. 2004. The role of cysteine residues as redox-sensitive regulatory switches. *Curr. Opin. Struct. Biol.* 14: 679–686.
40. Salmeen, A., and D. Barford. 2005. Functions and mechanisms of redox regulation of cysteine-based phosphatases. *Antioxid. Redox Signal.* 7: 560–577.
41. Sumimoto, S., M. Kawai, Y. Kasajima, and T. Hamamoto. 1992. Increased plasma tumour necrosis factor-alpha concentration in atopic dermatitis. *Arch. Dis. Child.* 67: 277–279.
42. Rullan, P., and J. Murase. 2009. Two cases of chronic atopic dermatitis treated with soluble tumor necrosis factor receptor therapy. *J. Drugs Dermatol.* 8: 873–876.
43. Jacobi, A., C. Antoni, B. Manger, G. Schuler, and M. Hertl. 2005. Infliximab in the treatment of moderate to severe atopic dermatitis. *J. Am. Acad. Dermatol.* 52: 522–526.